Hybrid front end interface DC-DC converter with ANFIS based control of EMS system

T.Vishnu kumar*1 ,V.Suresh kumar2, S.Arunraj

*[1]*Electrical and Electronics Engineering, K.Ramakrishnan college of technology, trichy, Tamilnadu, India*

vishnu341@gmail.com

[2]*Electrical and Electronics Engineering, K.Ramakrishnan college of technology, trichy, Tamilnadu, India*

vskped@gmail.com

[3]*Electrical and Electronics Engineering, K.Ramakrishnan college of technology, trichy, Tamilnadu, India*

sarunraj1712@gmail.com

Abstract- In this paper, the voltage regulation problem associated with mode switching in low voltage hybrid system has been addressed .This paper presents a hybrid zero voltage-switching (ZVS) isolated front end interface dc–dc converter which combines a boost half bridge (BHB) cell and a full-bridge (FB) cell, so that two different type of power sources, i.e., both current fed and voltage fed, can be combined togetherly by the proposed soft switched converter for various applications, such as pv cell and wind energy. By using two high-frequency transformers and a combined leg of switches, number of switches and gate driver circuits can be minimized. By phase-shift control, the converter can achieve ZVS turn-on of active switches and zero-current switching (ZCS) turn-off of diodes. In this paper, derivation, analysis, and design of the proposed converter are presented. Intelligent Adaptive Neuro-Fuzzy Inference System (ANFIS) based supervisory EMS(Energy Management System) controls the charge/ discharge of the energy storage system (ESS) when there is voltage changes to cooperate with ANFISPID in point of common coupling(PCC) voltage regulation. Finally, a 5–10V input, 600–700Voutput prototype with a 600W nominal power rating is built up and tested to demonstrate the effectiveness of the proposed converter topology.

Key words: Zero voltage switching, Zero current switching, Energy Management system, Adaptive Neuro fuzzy interference System.

I.INTRODUCTION

The efficiency of the power grid can be increased by connecting the renewable resources in hybrid manner [1]. In terms of the applications with a galvanic isolation, various system configurations have been investigated in the last decade, and usually they can be divided into three categories, i.e., direct hybridization, multiple-stage conversion and multiple-port conversion. The main disadvantage of this system is that if one input source is connected, only one converter will be operated and the other one will be completely under the idle condition that will reduce the power density of the whole system. Due to this reason, multi-port converters have been proposed and received

more and more attention in recent years. With different specifications and requirements, the adequate converter and/or configuration can be adopted.

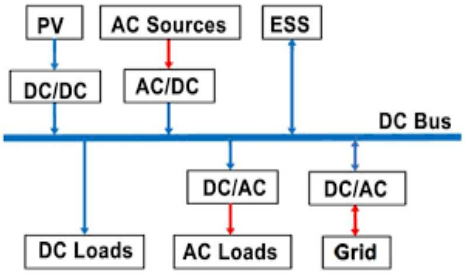

Fig 1: General DC grid system

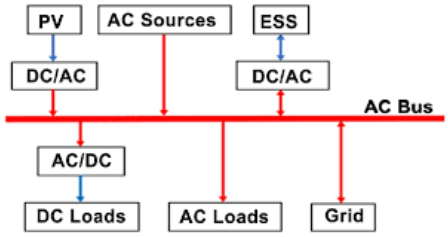

Fig 2: General AC grid system

Power distribution systems are undergoing substantial changes because of the new advents and technologies such as integration of large-scale renewable distributed generators (DGs)[3], advanced control & communication schemes and storage capable loads. Integration of large-scale renewable DGs in traditional power system is being popular day by day because of its capability to satisfy ever increasing energy demands, increased power quality, zero carbon emission and expandability.

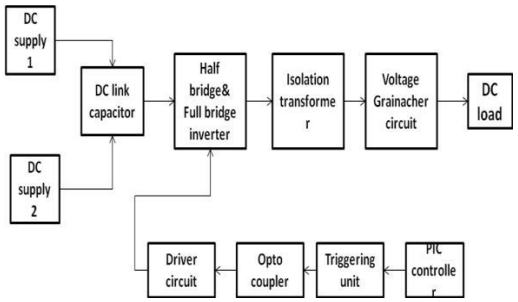

Fig 3: Block diagram of Proposed hybrid coverter

The salient advantages of the proposed converter can be summarized as follows:

1) Ability of dual-input connection;
2) Reduced number of power devices and their associated gate driver components;
3) ZVS turn-on of the main switches;
ZCS turn-of of the diode switch out reverse recovery issue.

II HYBRID FRONT END CONVERETER

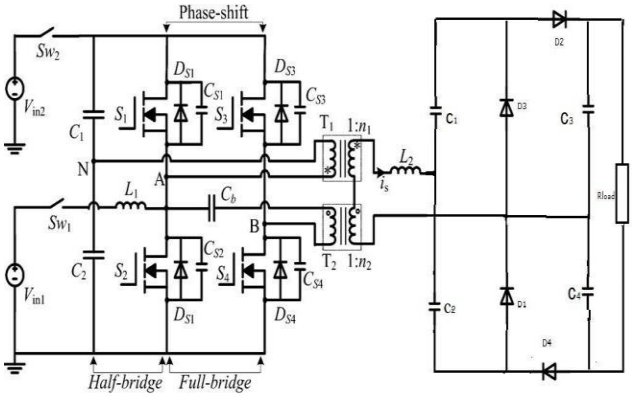

Fig 4: proposed hybrid converter

Mode 1:

During [t0 ,t2], as shown in Figure 3.3, the body diodes of S1 and S4 conduct and Vp is clamped to a voltage of 2VL until is decreases with a slope (2VL + VH)/L2 to zero at t2 .At t0 ,S1 turns ON under ZVS.

Mode 2:

During [t2, t3], when Is becomes positive and flows through D1, S1 and S4 will conduct and is increases with a slope (2VL − VH)/L2.

Mode 3:

During [t3, t5], when S4 turns OFF at t3, CS3 and CS4 start to resonate with L2 until VCS3 = 0, and then S3 can turn ON under ZVS. Current in the primary side flows through S1 and DS3 that makes Vp equal to VL, and is decreases with a slope (V − V)/L.

A voltage doubler circuit is employed on the secondary side and the voltage ringing over the diodes can inherently be clamped by the output capacitor C3 or C4 . L2 is essentially the sum of the transformer leakage inductance and an extra inductance. A dc blocking

capacitor Cb is added in series with the primary winding of T2 in order to avoid trans-former saturation caused by any asymmetrical operation in the FB circuit.

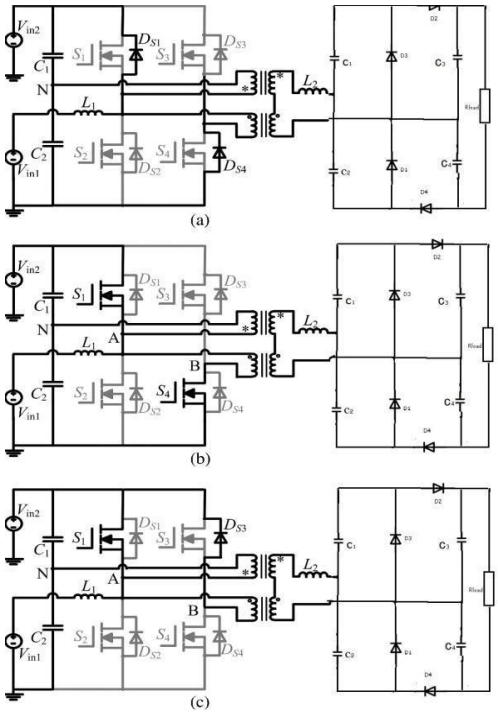

Fig 5: modes of operation

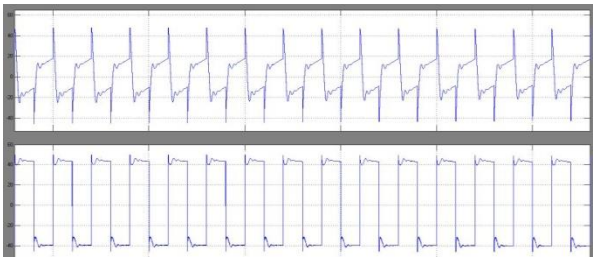

Fig 6: Output of BHB and FB Circuit

In this paper, only the symmetrical operation condition, i.e., the switching duty cycle D is 50%, is discussed, so that S1 and S2 as well as S3 and S4 have the complementary driving signals that gives Vin2 = 2Vin1 . Accordingly output voltage and power transferred can only be regulated by the phase-shift angle α of the two poles of the input bridge. The power factor of the high frequency ac loop can be evaluated by the angle ϕ which represents the phase delay between the secondary voltage and current. In order to avoid high reactive power in the converter, the regulated phase-shift angle will be limited in the range: $0 \le \alpha \le \pi$, in the practical applications.

Since the output diode rectifier is current driven, the following constrains must be satisfied: 1) when Is is positive, vs must be positive; and 2) when Is is negative, vs must be negative, and thereby based on the waveforms shown in the Fig. 4(a), the operation principle of the converter can be explained as follows. During [t0 , t2], as shown in Fig. 5(a), the body diodes of S1 and S4 conduct and Vp is clamped to a voltage of 2VL until is decreases with a slope (2VL + VH)/L2 to zero at t2 . At t0 , S1 turns ON under ZVS. During [t2 , t3], when is becomes positive and flows through D1 , S1 and S4 will conduct and is increases with a slope (2VL − VH)/L2 , as shown in Fig. 5(b). During [t3 , t5], when S4 turns OFF at t3 , CS 3 and CS 4 start to resonate with L2 until VC S 3 = 0, and then S3 can turn ON under ZVS. Current in the primary side flows through S1 and DS 3 that makes vp equal to VL , and is decreases with a slope (VH − VL)/L2 . The equivalent circuit is given in Fig. 5(c).

After t5 the second half switching cycle starts. Obviously, the diodes on the secondary side will always turn OFF under ZCS in the whole operation range. From the typical waveforms in fig 4(a) the defined peak current values I1 and I2 are given as

$$I_1 = i_s(t3) = \frac{2VL - VH}{L2} \cdot \frac{(\alpha - \varphi)T_s}{2\pi} \rightarrow 1$$

$$\rightarrow 2 \quad I_2 = i_s(t5) = \frac{2VL + VH}{L2} \cdot \frac{(\varphi)T_s}{2\pi}$$

$$\rightarrow 3 \quad I1 - I2 = \frac{VH - VL}{L2} \cdot \frac{(\pi - \alpha)T_s}{2\pi}$$

To determine the value of phase delay we can solve (3) for ϕ rad.

$$\Phi = 1/4(\pi + \alpha - VH/VL\ \pi) \rightarrow 4$$

Substituting (4) into (1) and (2), the output power of the pro- posed converter can be expressed

$$P_o = f(\alpha) = \begin{cases} \frac{V_H V_L}{4\omega L_2}\left(1-\frac{V_H^2}{V_L^2}\right), & 0 \le \alpha \le \varphi \\ \frac{V_H V_L \pi\left[-3\left(\frac{\alpha}{\pi}\right)^2+6\left(\frac{\alpha}{\pi}\right)+\left(1-\frac{V_H^2}{V_L^2}\right)\right]}{8\omega L_2}, & \varphi < \alpha \le \pi \end{cases}$$

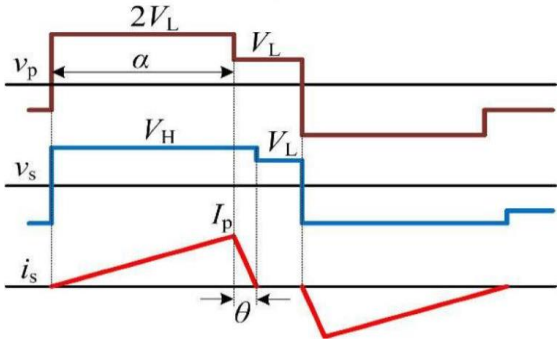

Fig 7: Typical waveforms under discontinuous I_s

III DESIGN CONSIDERATIONS

Generally, ZVS can be deduced on the precondition that the anti parallel diode of switch must conduct before the switch is triggered. In other words, the main devices are turned OFF with a positive current flowing and then the current diverts to the opposite diode which allows the in-coming MOSFET to be switched on under zero voltage. There for ZVS constraints depend on the magnitude of primary side currents ie.,(n1+n2).is,IL1 and n2 .is and have the relationships at driving instant.

-(n1+n2).is(t1)-iL1(t1)<0, for S1

(n1+n2).is(t5)-iL1(t5)>0 for S2

(n2).is(t3)>0 for s3,s4

The voltage gain versus phase-shift angle α is plotted in Fig. 6 under the conditions: Vin1 = 25 V, Vin2 = 2•Vin1 = 50 V, L2 = 40 μH, n1 = 4, n2 = 2, load resistance R = 300 Ω, and switching frequency fs = 100 kHz. It is clear that the results from calculation and simulation (MATLAB/PLECS is adopted

If we assume the switching frequency is constant, apparently (10) may not be satisfied when a larger input filter inductance L1 is employed, and furthermore the ZVS range as a function of α and L2 with different loads can be illustrated in Fig. 8. It can be found that increasing L2 and/or decreasing R can enlarge the ZVS region at the cost of the reduced power delivering capability.

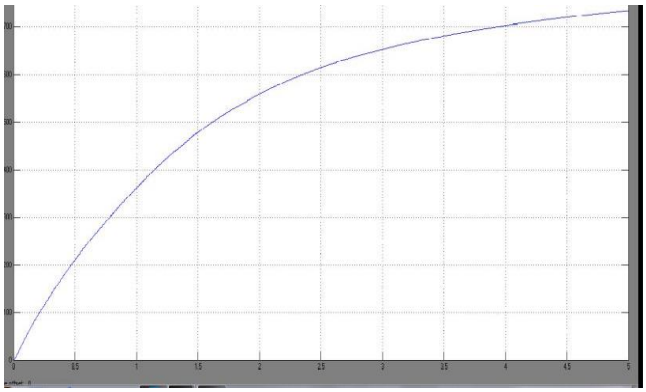

Fig 8:output of the hybrid interface converter

For converters with low input voltage and high current, turn- off loss of the switches on the low voltage side is the predominating factor of the switching loss [2], which cannot be ignored and is closely related to the stress of switch-off current. More-over, during converter design, it is also necessary to compute the root mean square (rms) values of the switch current to estimate conduction loss as for choosing MOSFETs, especially for the power devices located in the high current path. As an example, when input voltage is 30 V, Fig. 9 plots the values of transient turn-off current and rms current of the devices on the primary side as a function of α. It can be seen that the current stress is not distributed equally and among the switches, S2 will have to handle highest current stress and also high conduction loss owing to the BHB structure. Both the turn-off transient cur- rent and the rms current of S2 are approximately proportional to the phase-shift angle that means for same output power, if α decreases, switching and conduction losses of S2 will become less, so as a result the system efficiency can be improved. Regarding to this fact as well as the ZVS operation, an optimal design and tradeoff between switching loss and conduction loss may be considered for the future research.

IV ENERGY MANAGEMENT SYSTEM

Currently, a large amount of renewable DGs are being connected with low voltage weak distribution networks which are posing significant impacts on the operation and protection of the system. Moreover, increased accommodation of renewable DGs introduces new dynamics which has significant adverse impacts on the voltage profile at PCC [3-10]. The three-phase grid connected renewable DG systems are generally composed of renewable energy sources such as solar PVs, wind turbines, fuel cells etc. integrated with grid. These renewable sources are naturally intermittent and the generation of power at any given time depends on uncontrollable and nonlinear natural elements (such as solar irradiation, wind speed etc.). As, the resistance to reactance ratio (R/X) is more than one for low voltage distribution networks, the impact of power injected by renewable DGs has significant influence on voltage profile of the feeders. For the steady state operation of the system, the voltage along the distribution feeder needs to be within a permissible limit. strategy for voltage regulation of low voltage systems with PVs. But, frequent charge/ discharge reduce the life span of ESS and the solo implementation of ESS for voltage profile enhancement needs excessively large capacity of batteries which is not economically feasible. In this scenario, the cooperative operation of both the PV inverter and ESS for voltage regulation can ensure enhanced performance. Moreover, as power injected by solar PVs is uncertain, utilization of ESS can improve the state of power availability, operability and degree of controllability of the system.

Currently, a large amount of renewable DGs are being connected with low voltage weak distribution networks which are posing significant impacts on the operation and protection of the system. Moreover, increased accommodation of renewable DGs introduces new dynamics which has significant adverse impacts on the voltage profile at PCC.

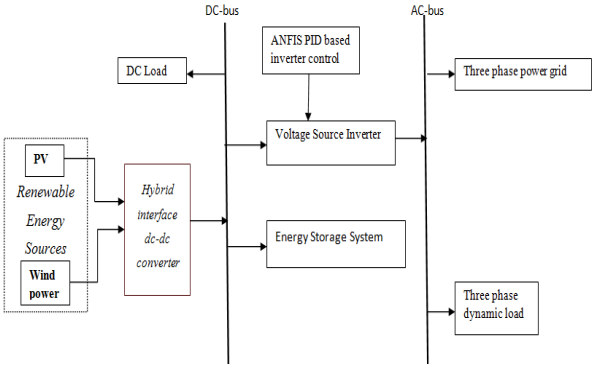

Fig 9: proposed control system

The three-phase grid connected renewable DG systems are generally composed of renewable energy sources such as solar PVs, wind turbines, fuel cells etc. integrated with grid. These renewable sources are naturally intermittent and the generation of power at any given time depends on uncontrollable and nonlinear natural elements (such as solar irradiation, wind speed etc.). PV inverter reactive power generation is limited and the impact of reactive power on PCC voltage of low voltage system is lesser due to higher R/X ratio. Utilization of ESS is another efficient strategy for voltage regulation of low voltage systems with PVs. But, frequent charge/ discharge reduce the life span of ESS and the solo implementation of ESS for voltage profile enhancement needs excessively large capacity of batteries which is not economically feasible. In this scenario, the cooperative operation of both the PV inverter and ESS for voltage regulation can ensure enhanced performance. Moreover, as power injected by solar PVs is uncertain, utilization of ESS can improve the state of power availability, operability and degree of controllability of the system .

Classical controllers like PID controllers are long-established in controlling the three-phase grid interfacing PV inverters. This control algorithm is widely used method in industrial automation because of its simplicity in structure and linear nature. However, this type of classical controllers require exact mathematical model of the system and are very sensitive to variation of operating conditions. If the PID gain

parameters are not selected properly, the response of the PID controller gets unstable, oscillatory or sluggish. So, it is necessary to tune the appropriate PID gains in real time in accordance with varying operating conditions to have stable and acceptable responses. Manual trial-and-error based tuning approaches would be very monotonous, expensive and time consuming and the tuned gains could become obsolete in a short time. As a result, conventional PID controllers may appear deficient as it is nearly impossible to set optimal gains due to rapid changes in dynamics of highly nonlinear grid-tied PV system environment which may result in large overshoot and system oscillation. In this situation, an adaptive intelligent system is necessary that can atomically tune the PID control parameters in accordance with system operating conditions in real time.

Fig 10: : General structure of ANFISPID-based control scheme

There are several intelligent control schemes that are being used for industrial automation in recent days like artificial neural networks (ANN), fuzzy inference system (FIS) or neuro-fuzzy systems. These intelligent control schemes do not require exact system model to operate and they are invulnerable to system dynamics. As a result, these intelligent controllers are advantageous in operating in highly nonlinear systems . Among the neuro-fuzzy models, ANFIS is easier to implement, faster, stronger in generalization skills and more accurate that inherits the learning and parallel data processing ability of artificial neural networks and inference ability (like human mind) of fuzzy inference system. As PID is already a well established and widely used control scheme in power industry, the combination of the simplicity of PID and the capability of ANFIS in handling the uncertainties has been proved to be advantageous while controlling the PV inverters under nonlinear operating conditions [15-20]. The proposed ANFIS-based intelligent PID control scheme adapts the nonlinear states of distribution system voltage profile and tunes the PID gain parameters automatically to improve the potential of PID control scheme in providing transient responses.

The reactive power capability of inverter interfaced DGs has been utilized for voltage regulation and enhancement of low voltage ride-through (LVRT) capability during grid faults in many literatures . Previously, some efforts have been made to incorporate fuzzy logic system to auto-tune PID control parameters. But, this approach involves laborious design steps such as manual tuning of membership functions, selection of fuzzy rules, selection of scaling factors etc. which are usually obtained by trial-and-error method. This turns it into a time consuming and error-prone process .

To our knowledge, this is the first time that a PID control scheme dynamically auto-tuned in real time by intelligent ANFIS has been implemented on PV inverter for regulating the PCC voltage of three-phase grid-tied solar PV system that shows robustness at any system worst-case scenarios. On the other hand, one reference has been found where ANFIS has been applied as a ‘supervisory controller’.

Figure 10 illustrates the general structure of the ANFISPID-based intelligent control scheme that has been developed and analyzed in this paper to control the grid interfacing three-phase PV inverter.

B. ANFIS-based supervisory energy management system design for ESS:

Connecting ESS with grid-tied solar PV system enhances the controllability, power

quality and reliability and it provides ancillary services such as voltage regulation support if proper EMS is applied .

Generally, the generated power from PV gradually increases and reaches to peak at midday and starts to decrease after that. The amount of surplus energy after satisfying the consumers depends upon the nonlinear behavior of the dynamic loads varying through the parts of the day and seasons of the year . In our study, an ANFIS-based supervisory EMS intelligently controls the charge/ discharge of ESS to balance the PV power generation and dynamic load demand that enhances the voltage support for the system (during short-term fluctuations too) by cooperating with PV inverter control scheme. This control scheme is advantageous over constant charging/ discharging rate strategy that may leave the storage capacity unused .

The structure of proposed ANFIS-based supervisory EMS has been illustrated in figure 10. It has three inputs. They are, the total power generated by solar PVs (P_{PV}), the total demand of the dynamic load connected with the grid-tied PV system ($P_{dynamic\ load}$) and the state of charge (SOC%) of the battery bank (ESS) [2]. SOC is the available capacity of ESS expressed as the percentage of the rated capacity. As output, the ANFIS-based supervisory EMS provides power references to the DC-DC buck-boost converter through which the battery bank is connected with the central DC bus. Several researchers have implemented classic state-based EMS to control the charge/ discharge states of ESS. The performance of the proposed ANFIS-based supervisory EMS for ESS has been compared with a classic state-based EMS. To prevent the battery bank from over-charging/ over-discharging, the SOC should be retained within appropriate allowable range. The ANFIS-based supervisory EMS prevents the ESS to be charged more than SOC_{max} (100% of rated storage capacity in this study) and to be discharged less than SOC_{min} (20% of rated storage capacity in this study) . Supervisory ANFIS has been trained with a set of data (70% training data, 15% testing data and 15% checking data) to emulate the proposed supervisory management system. Initial fuzzy inference system structure was generated by grid partitioning technique on the training data. A hybrid method that combines the least squares estimation method and back propagation method tunes the membership function parameters. Triangular membership function has been used for each of the three inputs.

A. Case 1: High PV generation during midday with low dynamic loads

In this case, the impact of high PV generation on the voltage profile at PCC during midday has been assessed. The impact of high PV generation has been illustrated in Figure 8 where per unit voltage at PCC exceeds the upper permissible limit (considering allowable voltage variation is 6% of the nominal voltage) from time= 330.59 seconds to 415.31 seconds, from time= 633.69 seconds to 754.42 seconds and again from time= 788.08 seconds resulted from the increase of excess power flowing back to grid.

The voltage profile at PCC after applying cooperative ANFISPID-based PV inverter control scheme and ANFIS-based supervisory control on ESS is illustrated.

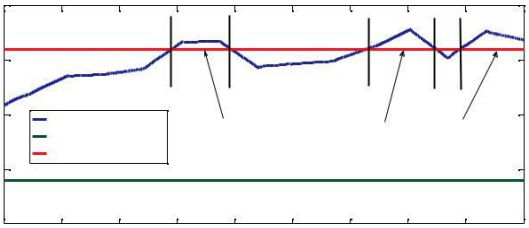

Fig. 11: Impact of high PV integration on PCC voltage during midday

ANFIS-based supervisory EMS system controls the charging and discharging of the ESS to store the excess energy and prevent it from flowing back to grid. The power delivered by PVs, dynamic load demand, power exchange with grid and the charged/ discharged power by ESS have been illustrated. When the ESS is being charged, the signing convention is negative and positive when it is discharging.

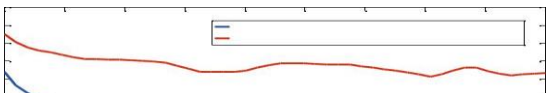

Fig 12: Reactive power absorbed by PV inverter during midday with and without cooperative ESS.

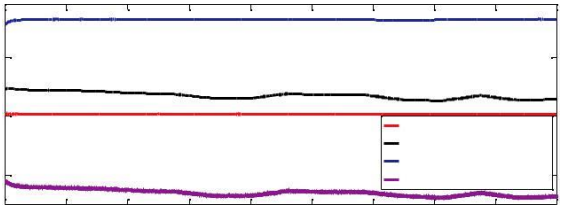

Fig. 13: (a) Per unit voltage at PCC when applying cooperative ANFISPID-based PV inverter control scheme and ANFIS-based supervisory EMS during midday (b) the power provided by PV (considering DC to AC derate factor 0.77), active power demand by dynamic loads, charged/ discharged power by ESS and power exchange with the traditional grid.

Figure 12 depicts the injected/ absorbed reactive power by PV inverter both in the presence and absence of cooperative ESS. It shows that necessary reactive power injection/ absorption gets lessened when ESS is implemented to cooperate simultaneously for voltage regulation.

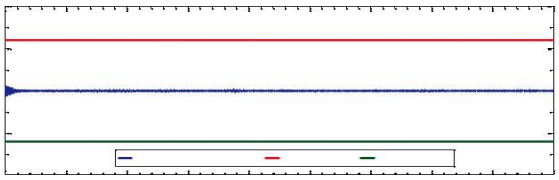

Fig. 14: Reactive power absorbed by PV inverter during midday with and without cooperative ESS.

If a classical PID with constant control parameters is applied on PV inverter for voltage regulation, it starts to provide oscillatory response due to dynamic changes in operating conditions. In figure 11, we can see that, classical PID starts to provide oscillatory response from time= 295 seconds while ANFISPID-based control scheme is showing robustness and keeping the PCC and DC bus voltage around its nominal value without oscillation.

B. Case 2: Low or no PV generation with evening peak loads

Figure 12 illustrates the voltage profile during evening when the PV generation is minimal and the consumer load is at peak. Voltage at PCC exceeds lower permissible limit and remains in non-permissible zone from time= 651 seconds to time= 800 seconds.

Fig. 15: Impact of low or no PV generation with evening peak load on PCC voltage

Fig. 15: Per unit voltage at PCC when applying cooperative ANFISPID-based PV inverter control scheme and ANFIS-based supervisory control on ESS during evening peak load (b) The Power provided by PV (considering DC to AC derate factor 0.77), active power demand by dynamic loads, charged/ discharged power by ESS and power delivered from grid during evening peak load.[4]

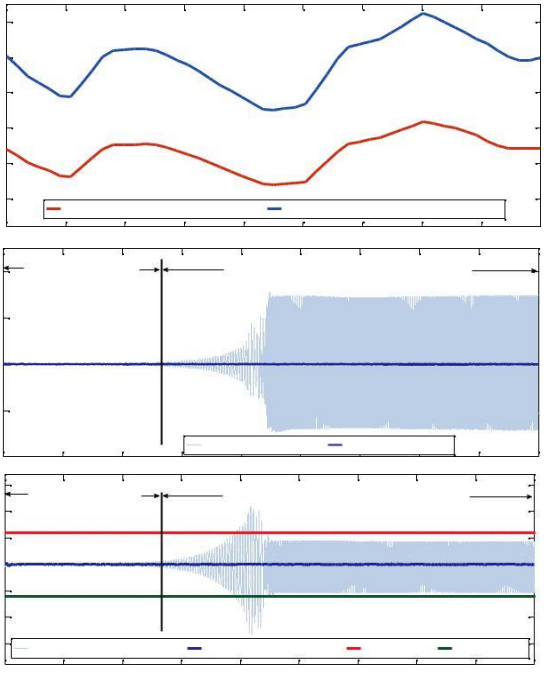

Fig. 16: Comparison of the proposed ANFISPID-based PV inverter control scheme with classical PID-based PV inverter control scheme for PCC (a) and dc-bus (b) voltage regulation during evening.

V CONCLUSION

In this proposed paper, a soft-switched isolated dc–dc converter with the ability of handling two independent inputs is derived, investigated, and

designed. Also ANFIS-based supervisory EMS has been implemented in this paper in real time to regulate the PCC voltage of weak distribution networks interconnected with large-scale PVs. Comparing to the existing topologies, the power converter proposed here has the advantages such as reduced number of switches, higher efficiency, and simple control. While, the main drawback is unequally distribution of current Stress among the power devices so that it will increase the design complexity. Case studies showed that the ANFIS-basedsupervisory EMS cooperates with ANFISPID-based PV inverter control scheme by minimizing PCC voltage deviation thus reducing necessary reactive power injection/ absorption by the inverter for voltage regulation. This reduces line losses through the system and overall expenses.

REFERENCES

[1]. T. Vishnu kumar, V. Suresh Kumar, "A new approach to front end interface DC-DC converter" International Journal of Multidisciplinary Research and Modern Education (IJMRME) ISSN(online): 2454-6119 Volume I, Issue II, 2015

[2]. V.Suresh kumar, T. Vishnu kumar, "A certain investigation for the battery charging system" International Journal of Multidisciplinary Research and Modern Education (IJMRME) ISSN(online): 2454-6119 Vol.1 Issue.1 2015

[3].S.Enimai, S.Jayanthi, T.Vishnu kumar "Isolated Power System Design Using Modified P&O Technique" Middle-East Journal of Scientific Research 24 (S2): 150-156, 2016, ISSN 1990-9233

[4] Ali, A. Nazar. "An ANFIS Based Advanced MPPT Control of a Wind-Solar Hybrid Power Generation System." International Review on Modelling and Simulations 7.ISSN 1974-9821 (2014): 638-643.

[5] .H. Tao, A. Kotsopoulos, J. L. Duarte, and M. A. M. Hendrix, "Transformer-coupled multiport ZVS bidirectional DC–DC converter with wide input range," IEEE Trans. Power Electron., vol. 23, no. 2, pp. 771–781, Mar. 2008

[6] .H. Krishnaswami and N. Mohan, "Three-port series-resonant DC–DC converter to interface renewable energy sources with bidirectional load and energy storage ports," IEEE Trans. Power Electron., vol. 24, no. 10, pp. 2289–2297, Oct. 2009.

[7].Z. Zhang, Z. Ouyang, O. C. Thomsen, and M. A. E. Andersen, "Analysis and design of a bidirectional isolated dc–dc converter for fuel cells and super-capacitors hybrid system," IEEE Trans. Power Electron., vol. 27, no. 2, pp. 848–859, Feb. 2012.

[8] Z. Zhang, O. C. Thomsen, M. A. E. Andersen, and H. R. Nielsen, "Dual- input isolated full-bridge boost DC-DC converter based on the distributed transformers," IET Power Electron., vol. 5, no. 7, pp. 1074–1083, Aug. 2012.

[9] C. Yoon, J. Kim, and S. Choi, "Multiphase DC-DC converters us- ing a boost-half-bridge cell for high-voltage and high-power applica- tions," IEEE Trans. Power Electron., vol. 26, no. 2, pp. 381–388, Feb. 2011.

[10] S. Jiang, D. Cao, Y. Li, and F. Z. Peng, "Gird-connected boost-half-bridge photoltaic microinverter system using repetitive current control and maxi- mum power point tracking," IEEE Trans. Power Electron., vol. 27, no. 11, pp. 4711–4722, Nov. 2012.

[11]. F. Krismer and J. Kolar, "Efficiency-optimized high current dual active bridge converter for automotive applications," IEEE Trans. Ind. Electron., vol. 59, no. 7, pp. 2745–2760, Jul. 2012.

[12] Z. Zhang, O. C. Thomsen, and M. A. E. Andersen, "Optimal design of a push-pull-forward half-bridge (PPFHB) bidirectional dc–dc converter with variable input voltage," IEEE Trans. Ind. Electron., vol. 59, no. 7, pp. 2761–2771, Jul. 2012.

[13] Zhang, B., et al. "An optimal and distributed method for voltage regulation in power distribution systems." *IEEE Transactions on Power Systems* 30.4 (2015): 1714-1726.

[14] Masters, C. L. "Voltage rise: the big issue when connecting embedded generation to long 11 kV overhead lines." *Power Engineering Journal* 16.1 (2002): 5-12.

[15] Quezada, V. M., Abbad, J. R., & Roman, T. G. S. "Assessment of energy distribution losses for increasing penetration of distributed generation." *IEEE Transactions on Power Systems*, 21.2 (2006), 533.

[16]Lopes, J. A., et al. "Integrating distributed generation into electric power systems: A review of drivers, challenges and opportunities." *Electric Power Systems Research* 77.9 (2007): 1189-1203.

[17] Chiradeja, P., and Ramakumar. R. "An approach to quantify the technical benefits of distributed generation." *IEEE Transactions on energy conversion* 19.4 (2004): 764-773.

[18]Mahmud, N., and Zahedi, A., "Review of control strategies for voltage regulation of the smart distribution network with high penetration of renewable distributed generation." *Renewable and Sustainable Energy Reviews* 64 (2016): 582-595.

[19]Zahedi, A. "A review of drivers, benefits, and challenges in integrating renewable energy sources into electricity grid." *Renewable and Sustainable Energy Reviews* 15.9 (2011): 4775-4779.

[20]Carvalho, P. M., Correia, P. F., & Ferreira, L. A. "Distributed reactive power generation control for voltage rise mitigation in distribution networks". *IEEE Transactions on Power Systems* 23.2 (2008): 766-772.

[21]Chen, Z., and Kong, W. "Protection Coordination Based on a Multi-agent for Distribution Power System with Distribution Generation Units." *International Workshop on Next Generation Regional Energy System Development*. (2007).